J. Phys. Chem. Solids Pergamon Press 1959. Vol. 10. pp. 35–43. Printed in Great Britain.

NEUTRON-DIFFRACTION STUDY OF ANTIFERROMAGNETIC $FeTiO_3$ AND ITS SOLID SOLUTIONS WITH α-Fe_2O_3*

G. SHIRANE
Westinghouse Research Laboratories, Pittsburgh, Pennsylvania

S. J. PICKART
Naval Ordnance Laboratory, White Oak, Maryland, and Brookhaven National Laboratory, Upton, New York

R. NATHANS
Pennsylvania State University, University Park, Pennsylvania, and Brookhaven National Laboratory, Upton New York

and

Y. ISHIKAWA
University of Tokyo, Tokyo, Japan

(*Received* 19 *November* 1958)

Abstract—While $FeTiO_3$ and α-Fe_2O_3 are both antiferromagnetic, some solid solutions of the two possess strong magnetic moments which are believed to be related to an ordering of the Fe and Ti atoms. Neutron powder patterns confirm the X-ray picture of $FeTiO_3$ as alternating layers of Fe and Ti along the [111] axis of the rhombohedral cell with intervening oxygen layers, and provide more accurate oxygen parameters. Data taken below the Néel point of 68°K suggest a model for the spin structure in which Fe^{2+} moments are ferromagnetically coupled within a (111) sheet and directed perpendicular to it. Studies on the solid solutions connect the presence of the spontaneous moment with ordering of the Ti and Fe atoms, and show that the spin arrangement in most of these compositions is of the α-Fe_2O_3 type with spins ferromagnetically coupled and lying within (111) sheets. The fact that no long-range ordered spin structure is observed down to 4·2°K for the sample containing 12 per cent hematite can be explained on the basis of an inhomogeneous magnetic structure.

1. INTRODUCTION

In recent years the magnetic properties of the $FeTiO_3$–α-Fe_2O_3 system have received considerable attention because of their importance in rock magnetism.[1–3] Though both the end members of this system are antiferromagnetic, strong magnetization was observed in some compositions on the $FeTiO_3$ side, and its existence was regarded as an important factor in determining the characteristics of the remanent magnetism in various rocks. A study of spin arrangement in this system by neutron diffraction seemed to be of special interest not only for its bearing on rock magnetism, but also for an understanding of magnetic interactions in this type of structure.

Both ilmenite, $FeTiO_3$, and hematite, α-Fe_2O_3, have the rhombohedral structure. α-Fe_2O_3 can be visualized as consisting of layers of Fe atoms in the (111) planes with oxygen layers between them. This is illustrated in Fig. 1, in which the cations *A* and *B* form alternate layers. It should be noticed that these cations are lying slightly above and below the plane of the layer, as shown schematically in Fig. 1(b). The structure of $FeTiO_3$ can be derived from that of α-Fe_2O_3 by replacing every other layer of Fe atoms by a layer of Ti atoms.

* This work was carried out in part at Brookhaven National Laboratory under the auspices of the Atomic Energy Commission and the National Security Agency.

Hematite exhibits a feeble ferromagnetism in addition to the fundamental antiferromagnetism below its Néel point of 950°K. An additional magnetic phase transition at 260°K was believed by NÉEL[4] to be a change of spin direction, which lies in the (111) plane above the transition temperature and along the [111] direction below it. This spin reorientation was confirmed by a neutron-diffraction study of SHULL *et al.*[5] who showed also that the spins are parallel within a given (111) plane and antiparallel between the adjacent planes. This structure may be written schematically as $(+\mathrm{Fe})_A(-\mathrm{Fe})_B(+\mathrm{Fe})_A$----, where A and B represent the different layers shown in Fig. 1.

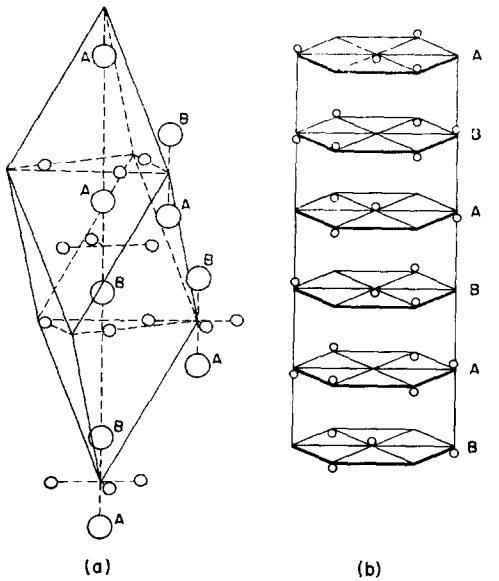

FIG. 1. The structure of $FeTiO_3$ and α-Fe_2O_3, showing (a) the rhombohedral and (b) the hexagonal unit cell. Circle A represents Fe, and B represents Fe in α-Fe_2O_3 and Ti in $FeTiO_3$. In ordered $FeTiO_3$–α-Fe_2O_3 solid solutions, A represents Fe and B represents Fe and Ti. Small circles in (a) are oxygens, which are omitted in (b).

The magnetic properties of ilmenite single crystals have recently been investigated by BIZETTE and TSAI.[6] Their measurements showed that $FeTiO_3$ is antiferromagnetic below a Néel temperature of 68°K and that the spin direction lies along [111]. Two models, which are shown in Fig. 4, have been proposed[3] for the spin arrangement. In one of these models (Fig. 4(c)) the spins are antiferromagnetically coupled within each layer; in the other (Fig. 4(a)) the spins are parallel to each other within a plane, but adjacent planes are antiparallel.

Finally, detailed studies of the magnetic properties of the solid solutions of these materials have been made by several investigators, working with both natural and synthesized compounds.[1,7,8] The Néel temperature of the system decreases almost linearly from 950°K for Fe_2O_3 to 68°K for $FeTiO_3$. Strong ferromagnetic moments were observed in the compositions on the $FeTiO_3$ side (see Fig. 2), and it was suggested that these moments result from a ferrimagnetic spin structure caused by ordering of the Fe and Ti atoms.

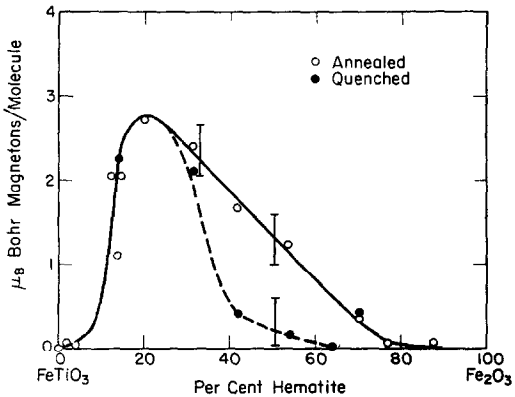

FIG. 2. The saturation moment of $(1-x)$ $FeTiO_3$–(x) Fe_2O_3 as measured by BOZORTH *et al.*[8] The moments estimated on the basis of the ordering parameter S, given by the neutron-diffraction data, are marked by vertical lines.

Additional evidence of this ordering is found in the fact that the magnetic moment of quenched samples was well below that of annealed samples near the composition 50 $FeTiO_3$–50 Fe_2O_3.[7–9]

The neutron measurements were carried out on synthesized powder specimens. Sample preparation consisted of placing the appropriate mixture of $FeTiO_3$ and α-Fe_2O_3 in an evacuated quartz tube (10^{-3} mm Hg) and quenching from 1200°C. Samples were maintained at this high temperature for at least 12 hr before quenching. Further details of the preparation and also the magnetic and electrical properties of the samples can be found in references (7) and (10). In addition to the end members, four solid solutions of varying compositions were prepared for the diffraction studies.

Their chemical composition is known to be within ± 2 per cent of the quoted values.

The actual sample of $FeTiO_3$ used had a Néel point of 55°K (from susceptibility measurements), which is somewhat lower than the 68°K reported for the natural crystal. In addition, the prepared sample had a slightly lower resistivity than that found in pure ilmenite,[10] where the observation of a high resistivity indicates the presence of iron in the form of Fe^{2+} and titanium as Ti^{4+}. Chemical analysis of the neutron sample showed it to contain a small amount of hematite (1·5 per cent). While it is not known definitely whether this α-Fe_2O_3 formed a solid solution, the persistence of a rather high resistivity suggests that the amount of Fe^{3+} and Ti^{3+}, if they are at all present, must be quite small. Consequently, in the calculations for $FeTiO_3$ the stoichiometric formula was used, along with the assumption of divalent iron and tetravalent titanium.

2. STRUCTURE OF $FeTiO_3$

The rhombohedral unit cell of $FeTiO_3$ contains two molecular units and the atomic positions can be described by the five parameters given in Table 1. (The parameters for α-Fe_2O_3 are shown in the same table for comparison.) The parameters for $FeTiO_3$ were determined by BARTH and POSNJAK,[11] using natural crystals. The ordering of Fe and Ti required by the space-group was clearly established by the difference in intensities of (210) and (120), which should be equal if Fe and Ti are distributed at random.

However, the small difference in scattering factors of Fe and Ti for X-rays made it difficult to determine whether Fe and Ti are perfectly ordered or not. Neutron intensities, on the other hand, are quite sensitive to this ordering, because of the negative scattering amplitude of Ti ($b = -0{\cdot}38 \times \times 10^{-12}$ cm) compared with that of Fe ($b = +0{\cdot}96 \times 10^{-12}$ cm). Obviously, this situation is considerably more favorable than the X-ray case, even though the powder technique is used for the neutron data.

Table 1. Structural parameters of $FeTiO_3$ and α-Fe_2O_3

The origin is chosen according to BARTH and POSNJAK[11] and differs from other choices,[5,15] including Fig. 1(a), by $(\frac{1}{4}, \frac{1}{4}, \frac{1}{4})$. Improved oxygen parameters obtained by the present work are given in parentheses.

$FeTiO_3$	α-Fe_2O_3
$R\bar{3}$ (C_{3i}^2)	$R\bar{3}C$ (D_{3d}^6)
$a = 5{\cdot}538$ Å $\alpha = 54°41'$	$a = 5{\cdot}424$ Å $\alpha = 55°17'$
2 Fe $\pm(u_1, u_1, u_1)$	4 Fe $\pm(u, u, u)$
2 Ti $\pm(u_2, u_2, u_2)$	$\pm(\frac{1}{2}+u, \frac{1}{2}+u, \frac{1}{2}+u)$
6 O $\pm(x, y, z)$	6 O $\pm(x, \frac{1}{2}-x, \frac{1}{4})$
$u_1 = 0{\cdot}358$	$u = 0{\cdot}355$
$u_2 = 0{\cdot}142$	
$x = 0{\cdot}555$	$x = 0{\cdot}542$ (0·550)
$y = -0{\cdot}055$ (−0·040)	
$z = 0{\cdot}250$ (0·235)	

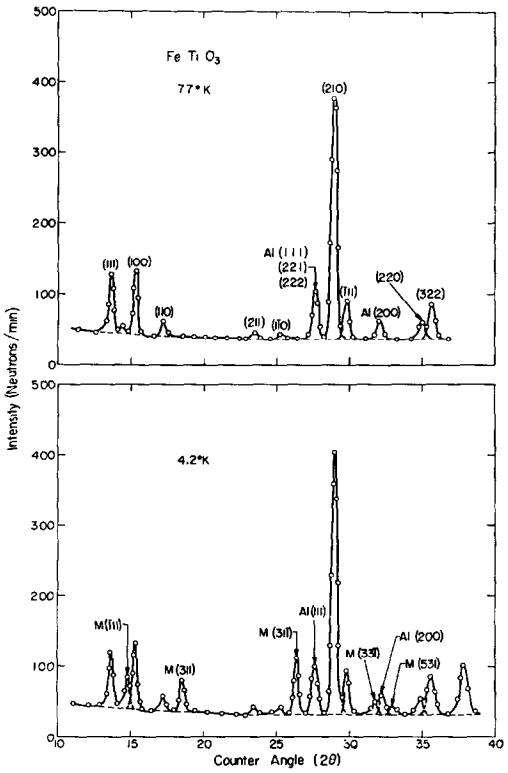

FIG. 3. Neutron-diffraction patterns of $FeTiO_3$ taken above and below the Néel point. The wavelength $\lambda = 1{\cdot}12$ Å.

It should be noted that the oxygen parameters given for $FeTiO_3$ satisfy the requirements of the higher symmetry of $R\bar{3}C$, that is, $y = (\frac{1}{2}) - x$ and $z = \frac{1}{4}$, though these are not necessary for $R\bar{3}$.

Table 2. Calculated and observed integrated intensities for $FeTiO_3$, relative to (210)

The data are taken at 4·2°K with a cylindrical sample. Magnetic intensities are calculated by using the scattering amplitude shown in Fig. 5(a).

hkl	Calculated intensities		Observed intensities
	(*a*) $S = 1{\cdot}0$, $x = 0{\cdot}555$, $y = -0{\cdot}055$, $z = 0{\cdot}250$	(*b*) $S = 0{\cdot}95$, $x = 0{\cdot}555$, $y = -0{\cdot}040$, $z = 0{\cdot}235$	
Nuclear			
(111)	231	211	190
(100)	274	218	195
(110)	28	45	44
(211)	19	16	18
(1$\bar{1}$0)	10	10	12
(210)(120)	800	800	800
($\bar{1}$11)	75	112	130
(200)	4	9	< 10
(220)	56	77	64
(322)	135	145	158
Magnetic (double cell)			
(111)		0	< 5
($\bar{1}$11)		73	68
(311)		88	87
(333)		0	< 5
(331)		0	< 5
(31$\bar{1}$)		157	162
(33$\bar{1}$)		29	25
(531)		33	36

Considering the fact that $u_2 = (\frac{1}{2}) - u_1$, which is again the requirement for $R\bar{3}C$, these oxygen parameters imply that Fe and Ti occupy crystallographically equivalent positions and are at the same distance from the surrounding oxygens. Since the ionic radius of Fe^{2+}(0·83 Å) is not identical with that of Ti^{4+}(0·64 Å), different bond distances might have been expected. For this reason, it appeared likely that the oxygen parameters could be improved, although the metal positions have been quite well determined by X-rays. Neutron diffraction can give more accurate oxygen parameters because the scattering amplitude of oxygen (0·58 × $\times 10^{-12}$ cm) is of the same order of magnitude as those of Fe and Ti. A refinement of the crystal structure was carried out in this direction, together with a determination of the magnetic spin arrangement below the Néel point.

Powder data taken on the ilmenite sample at 77 and 4·2°K are plotted in Fig. 3; the nuclear intensities of both runs agree satisfactorily. Calculations were first made from the parameters given by BARTH and POSNJAK,[11] which gave a reasonably good agreement with the observed nuclear intensities (see Table 2(a)). However, a careful comparison of observed and calculated values revealed a systematic difference which suggested that the ordering of Fe and Ti may not be complete. It was also clear at this stage that there was little room for improvement of the metal parameters u_1 and u_2. An attempt was made to improve the agreement between calculated and observed intensities by introducing three oxygen parameters and adjusting S, the ordering parameter. S is defined as the fraction of Ti at $\pm$ (u_2, u_2, u_2), which correspond to the B layer in Fig. 1, and ranges from unity for complete order to one-half for complete disorder. Systematic study led to the following parameters for the best fit:

$S = 0{\cdot}95 \quad x = 0{\cdot}555 \quad y = -0{\cdot}040 \quad z = 0{\cdot}235.$

According to the Goldschmidt radii, the Fe–O and Ti–O distances should be 2·15 and 1·96 Å respectively. The new oxygen parameters give Fe–O distances of 2·15 and 2·03 Å and Ti–O distances of 2·14 and 1·92 Å, and therefore result in more reasonable bond distances than the previous ones. It should be stressed, however, that the small number of reflections available for a determination of the parameters leaves some uncertainty in the final values.

The powder data taken below the Néel temperatures show several lines of magnetic origin in addition to the nuclear scattering (see Fig. 3). Indexing of these lines requires a doubling of the rhombohedral unit cell, and all of the observed lines can be indexed with h, k, and l all odd. Furthermore, no magnetic reflection was observed at (111) of the new unit cell, which implies that the spin direction is along [111], in agreement with the magnetic measurements by BIZETTE and TSAI.[6]

As can be seen in Fig. 1, the arrangement of the metal atoms in $FeTiO_3$ and α-Fe_2O_3 is such that it can be conveniently represented by a hexagonal lattice. Using such a cell for the magnetic structure and transposing the indices to the new representation, one finds that the hexagonal lattice must be doubled only along the main axis and not in the basal plane. The new hexagonal unit cell dimensions are:

$$a = 5{\cdot}09 \text{ Å} \qquad c = 28{\cdot}16 \text{ Å}.$$

The magnetic unit cell then contains 12 Fe atoms distributed in six layers. Among the several possible spin configurations, only the three models shown in Fig. 4(a)–(c) have plausible arrangements. These three are those obtained by considering three possible sequences of sign along the hexagonal axis, i.e. $(+\ -\ -\ +)$, $(+\ +\ -\ -)$, and $(+\ -\ +\ -)$. The spins in model (a) are coupled ferromagnetically within the same layer. On the other hand, the models (b) and (c) have antiparallel spin arrangements within the same layer. The models (a) and (c) correspond to the two models previously proposed, while the model (b) has not yet been considered.

Model (c) can be immediately excluded because it disagrees with the observed doubling of the unit cell. The intensities calculated on the basis of model (b) show poor agreement with the observed values, but satisfactory agreement is obtained with

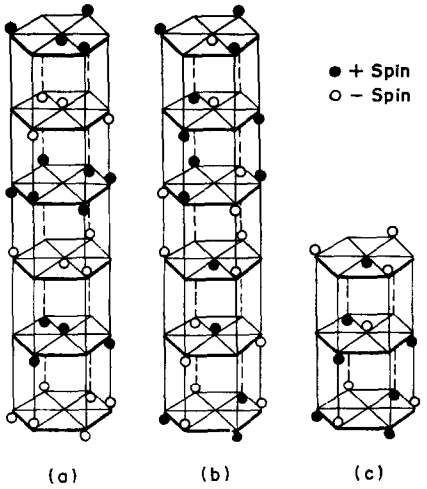

FIG. 4. Three possible magnetic structures for ilmenite, $FeTiO_3$. The Ti layer is omitted (see Fig. 1).

model (a). The calculated intensities are systematically smaller than the observed values, but this discrepancy can be removed by the assumption of orbital contribution to the magnetic moment of Fe^{2+}, as was observed in both FeO[5] and FeF_2.[12] The effect of an orbital contribution is not only to raise the moment value of Fe^{2+}, but to produce a magnetic form factor which falls off less rapidly with Bragg angle than that of Fe^{3+}, which was used

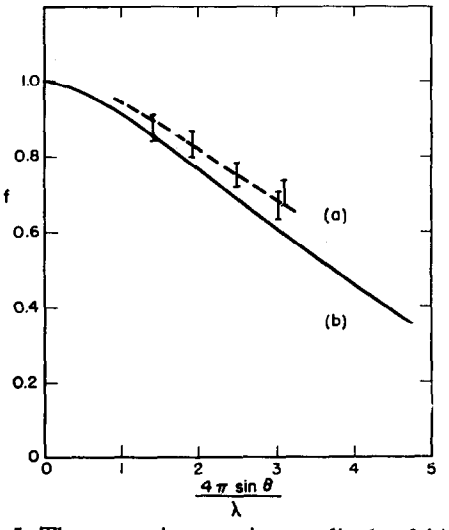

FIG. 5. The magnetic scattering amplitude of (a) Fe^{2+} in $FeTiO_3$, normalized to a value $1{\cdot}08 \times 10^{-12}$ cm and (b) Fe^{3+} in $MgFe_2O_4$,[13] normalized to $1{\cdot}26 \times 10^{-12}$ cm.

in the calculations. Fig. 5 is a plot of the observed magnetic scattering amplitude as a function of $\sin\theta/\lambda$, together with the normalized values for Fe^{3+} obtained by CORLISS *et al.*,[13] in their measurements on $MgFe_2O_4$. The observed and calculated intensities are compared in Table 2, where the magnetic component was calculated by using the amplitude of Fe^{2+} shown by the broken line in Fig. 5.

It should be borne in mind that the lack of complete ordering of the Fe and Ti atoms requires the partial occupation of the Ti layer by Fe, which may have an important bearing on the magnetic ordering of the spins. Although the neutron data can in principle give the average moment on the Ti layer, its contribution to the total magnetic intensity for this small amount of disorder is too small to be evaluated quantitatively.

3. STRUCTURE OF $(1-x)$ $FeTiO_3$–(x) Fe_2O_3

In the solid solutions the two questions that must be answered are the nature of the magnetic spin arrangement and the dependence of the Fe–Ti ordering, or the quantity S, on composition and heat treatment. Four compositions of the solid-solution system $(1-x)$ $FeTiO_3$–(x) Fe_2O_3, with $x = 0{\cdot}12$, $0{\cdot}33$, $0{\cdot}50$ and $0{\cdot}70$, were studied. In addition, a sample of pure α-Fe_2O_3 was investigated in order to verify the spin structure previously reported by SHULL *et al.*[5] The data, taken with somewhat improved resolution, are satisfied by their model. In giving a spin arrangement in α-Fe_2O_3, one should note that the neutron powder data are independent of any specific direction for the spin within the (111) planes. The best agreement for the nuclear intensities was obtained by adjusting the oxygen parameter to 0·550 from the reported value of 0·542.[14]

Room-temperature patterns were taken on all four mixed compounds. In addition, the sample with $x = 0{\cdot}12$ was run at liquid-helium temperature, since the magnetic transition of this compound is below room temperature. In no case was there any evidence of superlattice reflections as found in $FeTiO_3$.

For the sample of composition $x = 0{\cdot}12$, no significant difference could be noted between the room-temperature data and that taken at 4·2°K, although the latter temperature is far below the quoted value of 170°K for the onset of ferromagnetic ordering.[7] The single exception was the presence of broad "humps" in the diffraction pattern near the positions of the (100) and (210) reflections, which are characteristic of short-range ordering (see Fig. 6). The absence of superlattice

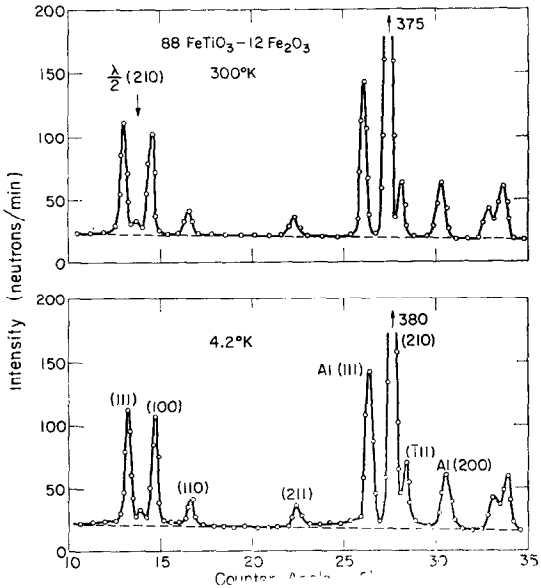

FIG. 6. Neutron-diffraction patterns of 88 $FeTiO_3$–12 Fe_2O_3 at 300 and 4·2°K. $\lambda = 1{\cdot}05$ Å.

reflections and the ordering of Fe and Ti known from the room-temperature data allow only model (c) in Fig. 4, but in that case there would be an appreciable magnetic contribution to the observed intensities for any possible direction of the spin. It may be concluded, therefore, that there is no long-range magnetic order in this compound, at least down to 4·2°K. A discussion of this result, which is somewhat surprising in view of the known ferromagnetic moment, will be deferred until the next section. In order to establish this behavior as not characteristic of the particular sample, a similar composition with $x = 0{\cdot}10$ provided by Dr. R. M. BOZORTH, of the Bell Telephone Laboratories, was also investigated at 77°K and it showed identical results.

The analysis of the compounds for $x \geqslant 0{\cdot}33$ is complicated by the large number of parameters to be determined from the relatively few observable lines. Since the data were taken below the Curie temperature, the degree of magnetic saturation

(σ_{RT}/σ_0) becomes an unknown, as well as S, the ordering parameter. Moreover, the results on $FeTiO_3$ raise the possibility of three oxygen parameters instead of one as in hematite. The data were analyzed in the following manner. Since the magnetic intensities were of the same nature as those found in α-Fe_2O_3 with no additional lines present, a model for the spin arrangement similar to that in hematite was adopted, that is, spins ferromagnetically coupled and lying within the (111) planes with adjacent planes antiparallel. The positional parameters of $FeTiO_3$ were used for compositions with $x < 0{\cdot}5$ and those of α-Fe_2O_3 for $x > 0{\cdot}5$. The

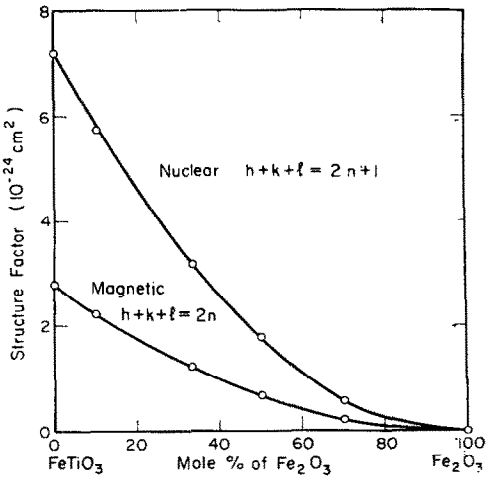

FIG. 7. Nuclear and magnetic structure factors as a function of composition for the perfectly ordered case (per two molecular units). The magnetic structure factors are calculated for $q^2 = 1$ and $f^2 = 0{\cdot}6$ ($\sin\theta/\lambda = 0{\cdot}25$).

order parameter S and the degree of saturation (σ_{RT}/σ_0) were then adjusted to secure the best agreement.

The intensities of the group of reflections with $h+k+l = 2n+1$ are proportional to $(b_A - b_B)^2$, where subscripts A and B refer to the layers shown in Fig. 1 and b_A is the sum of the nuclear scattering amplitude of atoms on the A layer. These intensities are very sensitive to the degree of order, but their absolute value for $S = 1$ decreases rapidly with increasing concentration of α-Fe_2O_3, as shown in Fig. 7. The value of the order parameter giving the best fit for the nuclear intensities in the $x = 0{\cdot}12$ and $0{\cdot}33$ compounds is $S = 0{\cdot}9$. For $x = 0{\cdot}50$, where the accuracy is less, S is found to lie between 0·5 (value for complete disorder) and 0·65. For the composition $x = 0{\cdot}70$ no estimate of the degree of order can be made, but it seems reasonable to assume that it is not greater than for $x = 0{\cdot}50$. It can be summarized that the ordering of Fe and Ti in quenched samples develops only when the concentration of $FeTiO_3$ in the solid solutions exceeds 50 per cent.

As mentioned earlier, the saturation moments of compositions near $x = 0{\cdot}50$ are strongly affected by heat treatment. It was assumed that this was related to an increased ordering of Fe and Ti ions brought about by the annealing. This point was directly tested by neutron diffraction with samples of composition $x = 0{\cdot}50$. After the diffraction data were collected with the quenched sample, the same sample was annealed by cooling slowly (10°/hr)

Table 3. Calculated and observed integrated intensities for quenched and annealed sample of 50 $FeTiO_3$–50 Fe_2O_3

The data are taken at 300°K.

(a) Quenched. Calculated with $S = 0{\cdot}50$ (disorder), $u = 0{\cdot}356$, $x = 0{\cdot}553$, $y = -0{\cdot}053$, $z = 0{\cdot}250$

hkl	Calculated intensities			Observed intensities
	Nuclear	Magnetic	Total	
(111)	0	321	321	321
(100)	0	190	190	176
(110)	132	0	132	125
(211)	250	0	250	234
(1$\bar{1}$0)	46	0	46	35
(210)	837	146	983	1038
($\bar{1}$11)	0	28	28	32

(b) Annealed. Calculated with $S = 0{\cdot}85$, $u = 0{\cdot}356$, $x = 0{\cdot}553$, $y = -0{\cdot}043$, $z = 0{\cdot}240$

hkl	Calculated intensities			Observed intensities
	Nuclear	Magnetic	Total	
(111)	54	321	375	400
(100)	43	190	233	262
(110)	159	2	161	150
(211)	220	7	227	229
(1$\bar{1}$0)	46	4	50	58
(210)	886	146	1032	971
($\bar{1}$11)	35	28	63	66

from 800°C to room temperature.[9] As a result of this heat treatment, the saturation moment at room temperature increased from 4 to 22 e.m.u./g (0·6μ_B per molecule), but no change in lattice constants was observed.

The neutron-diffraction intensities taken with this annealed sample are compared in Table 3 with the data on the same sample in the quenched state. A definite increase in intensity was observed in (100) and ($\bar{1}$11) and, to a lesser extent, in (111). These differences can be accounted for qualitatively by assuming an increased order of Fe and Ti, but better agreement can be obtained if the oxygen parameters are changed from the α-Fe_2O_3 type to the $FeTiO_3$ type, as shown in the table. This result is reasonable, since one might expect the ordering of Fe and Ti to be accompanied by a rearrangement of oxygen positions. Though the increased order ($S = 0{\cdot}85$) and associated change of oxygen parameters are definitely established, the final value of parameters must be taken with some reserve because of the small number of lines available for analysis.

With regard to the magnetic structure, one finds that the magnetic reflections can be divided into two groups:

$$F^2 \sim (p_A - p_B)^2 \text{ for } h+k+l = 2n+1,$$

$$F^2 \sim (p_A + p_B)^2 \text{ for } h+k+l = 2n,$$

where suffixes A and B refer to A and B layers. In the first case, since the spin direction in the B layer is opposite to that of the A layer, $(p_A - p_B)^2 = (|p_A| + |p_B|)^2$, and there arises a large contribution to the intensity which can be established without any difficulty. These reflections, however, do not provide information on how the spins are distributed between A and B layers, and equal intensities are obtained as long as they are parallel within the same layer and the total moment is the same.

The second group of lines with $h+k+l = 2n$ should show how the spins are distributed in A and B layers. However, the intensities of this group are not very strong, as can be seen in Fig. 7, where the most favorable case with $q^2 = 1$ is taken. Moreover, the trigonometric part of the structure factor is not very large for reflections observed in the forward direction (see Table 3(b)). Therefore, it is not possible to draw any conclusion from these lines for compositions with $x \geqslant 0{\cdot}33$. However, the distribution of Ti and Fe atoms in the two layers has already been determined by the nuclear scattering, so that the only remaining ambiguity is how Fe^{3+} and Fe^{2+} are distributed between the two layers.

4. DISCUSSION

In summary, there are in the $FeTiO_3$–α-Fe_2O_3 series two distinct magnetic structures. One of these is that observed in ilmenite and is shown as model (a) in Fig. 4; the other, a modified form of the hematite structure, can be easily visualized from Fig. 1. In this structure one of the layers is occupied mostly by Fe atoms and the other by Ti and Fe atoms; the spins are parallel within the layer and adjacent layers are antiparallel. The amount of order developed between Ti and Fe atoms depends on the fraction of hematite in the sample and, for certain concentrations, on the heat treatment.

Because of the small amount of disorder found in $FeTiO_3$, it is difficult to say very much concerning the type of interactions responsible for the ordering scheme. Li's suggestion[15] that magnetic Ti^{3+} ions in the layer separating the Fe^{2+} are needed to propagate the order would seem to be ruled out, since it predicts a magnetic lattice unlike the one observed. The possible role of the Fe on the Ti layer is unknown, however, and the question also arises as to whether the ordering is stabilized by the slight impurity of hematite present in the sample. These points are best discussed in relation to the phenomena observed in the compound containing 12 per cent hematite.

In spite of the fact that the sample with $x = 0{\cdot}12$ had a measured moment of about 1μ_B/molecule, the neutron data for this composition indicated no long-range magnetic order far below the ferromagnetic Curie point. The explanation for this apparent inconsistency may be sought in the magnetic structure of $FeTiO_3$. The required doubling of the unit cell means that an antiferromagnetic coupling must exist between two widely separated iron layers (at least 4·0 Å apart). If a small amount of Fe on the intervening Ti layer is the means by which the over-all antiferromagnetic order is propagated, one would not expect the addition of slightly more Fe to cause the observed destruction of the long-range order. Rather, if a weak superexchange coupling between the Fe^{2+} ions on

alternate layers is responsible for the antiferromagnetism, then the introduction of a certain amount of Fe^{3+} on the intermediate Ti layer may quite conceivably alter the Néel point. The much stronger interaction between the Fe^{2+}–Fe^{3+} on adjacent layers will tend to define the spin configuration in the immediate vicinity of an Fe^{3+} ion, thus effectively lowering the number of magnetic neighbors (and the transition temperature) of the $FeTiO_3$ type of ordering. Upon further substitution of Fe^{3+}, a point will be reached where the coupling between neighboring layers is able to produce a short-range order, forming ferrimagnetic clusters which are not sufficient in extent to produce coherent diffraction peaks but can result in an observable over-all moment. Evidence for these clusters is found in the broad "humps" in the low-temperature pattern for $x = 0{\cdot}12$, which occur near the Bragg angles where strong magnetic reflections are observed for the ordered ferrimagnetic structures. This explanation accounts for the initial lowering of the Néel point, for the minimum addition of hematite required before a magnetic moment is observed (nearly 5 per cent according to the magnetic data), and for the subsequent increase in the saturation moment and Curie point with the addition of more iron. The picture of local fluctuations in the magnetic structure has already been used by NÉEL[16] and by GRIMES *et al.*,[17] to explain the magnetic moments and specific heats of solutions of an antiferromagnetic and a ferrimagnetic ferrite.

The distribution in the solid solutions of the Fe^{2+} and Fe^{3+} atoms between the different layers remains unsolved. However, assuming that both valence states are positioned at random on the two layers, and using the neutron values for the ordering parameter S, one can calculate the expected moment. If the Fe^{2+} ions are assumed to be confined to the A layers, the calculated moments become smaller by approximately 10 per cent. The results are compared with the saturation moments measured by BOZORTH *et al.*[8] in Fig. 2. In both cases, the calculated and experimental points agree within the uncertainty of the measurement of S.

Finally, it should be mentioned that the values of σ_{RT}/σ_0 found from the neutron data are in disagreement with those calculated from the magnetic measurements. For the compositions with $x = 0{\cdot}33$ and $0{\cdot}50$, σ_{RT}/σ_0 was found to be $0{\cdot}4$ and $0{\cdot}75$, respectively, while the curves of saturation magnetization versus temperature[7] are nearly linear and yield values of $0{\cdot}3$ and $0{\cdot}5$. The neutron values are more typical of a Brillouin function than the magnetization data. Since the quantity measured by neutron diffraction is $|\sigma_A|+|\sigma_B|$ and the magnetic moment depends on $|\sigma_A|-|\sigma_B|$, a difference in the temperature-dependences of σ_A and σ_B could explain the observed discrepancy. Further study of the temperature-dependence of the magnetic intensities may be desirable to confirm this point.

Acknowledgements—The authors wish to thank Dr. R. M. BOZORTH, of the Bell Telephone Laboratories, for supplying the sample for comparison, and Dr. J. S. KASPER, of the General Electric Research Laboratory, for discussion concerning the parameters found in his unpublished work on the α-Fe_2O_3–Cr_2O_3 system.

REFERENCES

1. NAGATA T., AKIMOTO S., and UYEDA S., *J. Geomagn. Geoelect., Kyoto* **5,** 168 (1953).
   NAGATA T. and AKIMOTO S., *Geofis. Pura Appl., Milano* **34,** 36 (1956).
2. NÉEL L., *Advances in Phys.* **4,** 191 (1955).
3. NICHOLLS G. D., *Advances in Phys.* **4,** 139 (1955).
4. NÉEL L., *Rev. Mod. Phys.* **25,** 58 (1953).
5. SHULL C. G., STRAUSER W. A., and WOLLAN E. O., *Phys. Rev.* **83,** 333 (1951).
6. BIZETTE H. and TSAI B., *C.R. Acad. Sci., Paris* **242,** 2124 (1956).
7. ISHIKAWA Y. and AKIMOTO S., *J. Phys. Soc. Japan* **12,** 834, 1083 (1957).
8. BOZORTH R. M., WALSH D. E., and WILLIAMS A. J., *Phys. Rev.* **108,** 157 (1957).
9. ISHIKAWA Y., *J. Phys. Soc. Japan* **13,** 828 (1958).
10. ISHIKAWA Y., *J. Phys. Soc. Japan* **13,** 37 (1958).
11. BARTH F. W. and POSNJAK E., *Z. Krist.* **88,** 265 (1934).
12. ERICKSON R. A., *Phys. Rev.* **90,** 779 (1953).
13. CORLISS L. M., HASTINGS J. M., and BROCKMAN F. G., *Phys. Rev.* **90,** 1013 (1953).
14. WYCKOFF R. W. G., *Crystal Structures* Vol. I. Interscience Publishers, New York (1948).
15. LI Y. Y., *Phys. Rev.* **102,** 1015 (1956).
16. NÉEL L., *C.R. Acad. Sci., Paris* **230,** 375 (1950).
17. GRIMES D. M., LEGVOLD S., and WESTRUM E. F., Jr., *Phys. Rev.* **106,** 866 (1957).